JOURNAL OF Applied Polymer SCIENCE

Special Issue: Microfiltration and Ultrafiltration Membrane Science and Technology

Guest Editors: Prof. Isabel C. Escobar (University of Toledo) and Prof. Bart Van der Bruggen (University of Leuven)

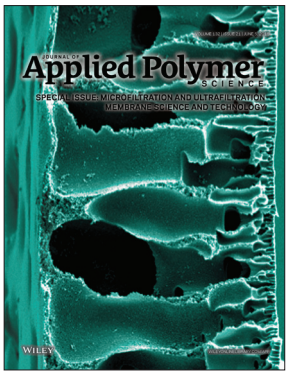

EDITORIAL

Microfiltration and Ultrafiltration Membrane Science and Technology
I. C. Escobar and B. Van der Bruggen, *J. Appl. Polym. Sci.* 2015, **DOI: 10.1002/app.42002**

REVIEWS

Nanoporous membranes generated from self-assembled block polymer precursors: *Quo Vadis*?
Y. Zhang, J. L. Sargent, B. W. Boudouris and W. A. Phillip, *J. Appl. Polym. Sci.* 2015, **DOI: 10.1002/app.41683**

Making polymeric membranes anti-fouling via "grafting from" polymerization of zwitterions
Q. Li, J. Imbrogno, G. Belfort and X.-L. Wang, *J. Appl. Polym. Sci.* 2015, **DOI: 10.1002/app.41781**

Fouling control on MF/ UF membranes: Effect of morphology, hydrophilicity and charge
R. Kumar and A. F. Ismail, *J. Appl. Polym. Sci.* 2015, **DOI: 10.1002/app.42042**

EMERGING MATERIALS AND FABRICATION

Preparation of a poly(phthalazine ether sulfone ketone) membrane with propanedioic acid as an additive and the prediction of its structure
P. Qin, A. Liu and C. Chen, *J. Appl. Polym. Sci.* 2015, **DOI: 10.1002/app.41621**

Preparation and characterization of MOF-PES ultrafiltration membranes
L. Zhai, G. Li, Y. Xu, M. Xiao, S. Wang and Y. Meng, *J. Appl. Polym. Sci.* 2015, **DOI: 10.1002/app.41663**

Tailoring of structures and permeation properties of asymmetric nanocomposite cellulose acetate/silver membranes
A. S. Figueiredo, M. G. Sánchez-Loredo, A. Maurício, M. F. C. Pereira, M. Minhalma and M. N. de Pinho, *J. Appl. Polym. Sci.* 2015, **DOI: 10.1002/app.41796**

LOW-FOULING POLYMERS

Low fouling polysulfone ultrafiltration membrane via click chemistry
Y. Xie, R. Tayouo and S. P. Nunes, *J. Appl. Polym. Sci.* 2015, **DOI: 10.1002/app.41549**

Elucidating membrane surface properties for preventing fouling of bioreactor membranes by surfactin
N. Behary, D. Lecouturier, A. Perwuelz and P. Dhulster, *J. Appl. Polym. Sci.* 2015, **DOI: 10.1002/app.41622**

PVC and PES-*g*-PEGMA blend membranes with improved ultrafiltration performance and fouling resistance
S. Jiang, J. Wang, J. Wu and Y. Chen, *J. Appl. Polym. Sci.* 2015, **DOI: 10.1002/app.41726**

Improved antifouling properties of TiO_2/PVDF nanocomposite membranes in UV coupled ultrafiltration
M. T. Moghadam, G. Lesage, T. Mohammadi, J.-P. Mericq, J. Mendret, M. Heran, C. Faur, S. Brosillon, M. Hemmati and F. Naeimpoor, *J. Appl. Polym. Sci.* 2015, **DOI: 10.1002/app.41731**

Development of functionalized doped carbon nanotube/polysulfone nanofiltration membranes for fouling control
P. Xie, Y. Li and J. Qiu, *J. Appl. Polym. Sci.* 2015, **DOI: 10.1002/app.41835**

JOURNAL OF Applied Polymer SCIENCE

Special Issue: Microfiltration and Ultrafiltration Membrane Science and Technology

Guest Editors: Prof. Isabel C. Escobar (University of Toledo) and
Prof. Bart Van der Bruggen (University of Leuven)

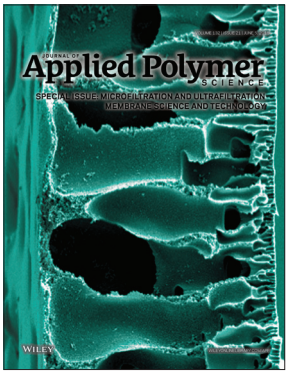

SURFACE MODIFICATION OF POLYMER MEMBRANES

Highly chlorine and oily fouling tolerant membrane surface modifications by *in situ* polymerization of dopamine and poly(ethylene glycol) diacrylate for water treatment
K. Yokwana, N. Gumbi, F. Adams, S. Mhlanga, E. Nxumalo and B. Mamba, *J. Appl. Polym. Sci.* 2015, **DOI: 10.1002/app.41661**

Fouling control through the hydrophilic surface modification of poly(vinylidene fluoride) membranes
H. Jang, D.-H. Song, I.-C. Kim, and Y.-N. Kwon, *J. Appl. Polym. Sci.* 2015, **DOI: 10.1002/app.41712**

Hydroxyl functionalized PVDF-TiO_2 ultrafiltration membrane and its antifouling properties
Y. H. Teow, A. A. Latif, J. K. Lim, H. P. Ngang, L. Y. Susan and B. S. Ooi, *J. Appl. Polym. Sci.* 2015, **DOI: 10.1002/app.41844**

Enhancing the antifouling properties of polysulfone ultrafiltration membranes by the grafting of poly(ethylene glycol) derivatives via surface amidation reactions
H. Yu, Y. Cao, G. Kang, Z. Liu, W. Kuang, J. Liu and M. Zhou, *J. Appl. Polym. Sci.* 2015, **DOI: 10.1002/app.41870**

SEPARATION APPLICATIONS

Experiment and simulation of the simultaneous removal of organic and inorganic contaminants by micellar enhanced ultrafiltration with mixed micelles
A. D. Vibhandik, S. Pawar and K. V. Marathe, *J. Appl. Polym. Sci.* 2015, **DOI: 10.1002/app.41435**

Polymeric membrane modification using SPEEK and bentonite for ultrafiltration of dairy wastewater
A. Pagidi, Y. Lukka Thuyavan, G. Arthanareeswaran, A. F. Ismail, J. Jaafar and D. Paul, *J. Appl. Polym. Sci.* 2015, **DOI: 10.1002/app.41651**

Forensic analysis of degraded polypropylene hollow fibers utilized in microfiltration
X. Lu, P. Shah, S. Maruf, S. Ortiz, T. Hoffard and J. Pellegrino, *J. Appl. Polym. Sci.* 2015, **DOI: 10.1002/app.41553**

A surface-renewal model for constant flux cross-flow microfiltration
S. Jiang and S. G. Chatterjee, *J. Appl. Polym. Sci.* 2015, **DOI: 10.1002/app.41778**

Ultrafiltration of aquatic humic substances through magnetically responsive polysulfone membranes
N. A. Azmi, Q. H. Ng and S. C. Low, *J. Appl. Polym. Sci.* 2015, **DOI: 10.1002/app.41874**

BIOSEPARATIONS APPLICATIONS

Analysis of the effects of electrostatic interactions on protein transport through zwitterionic ultrafiltration membranes using protein charge ladders
M. Hadidi and A. L. Zydney, *J. Appl. Polym. Sci.* 2015, **DOI: 10.1002/app.41540**

Modification of microfiltration membranes by hydrogel impregnation for pDNA purification
P. H. Castilho, T. R. Correia, M. T. Pessoa de Amorim, I. C. Escobar, J. A. Queiroz, I. J. Correia and A. M. Morão, *J. Appl. Polym. Sci.* 2015, **DOI: 10.1002/app.41610**

Hemodialysis membrane surface chemistry as a barrier to lipopolysaccharide transfer
B. Madsen, D. W. Britt, C.-H. Ho, M. Henrie, C. Ford, E. Stroup, B. Maltby, D. Olmstead and M. Andersen, *J. Appl. Polym. Sci.* 2015, **DOI: 10.1002/app.41550**

Membrane adsorbers comprising grafted glycopolymers for targeted lectin binding
H. C. S. Chenette and S. M. Husson, *J. Appl. Polym. Sci.* 2015, **DOI: 10.1002/app.41437**

Journal of Applied Polymer Science

Low fouling polysulfone ultrafiltration membrane via click chemistry

Yihui Xie, Russell Tayouo, Suzana Pereira Nunes
Water Desalination and Reuse Center, King Abdullah University of Science and Technology (KAUST), Kingdom of Saudi Arabia
Correspondence to: S. P. Nunes (E-mail: suzana.nunes@kaust.edu.sa)

ABSTRACT: Hydrophilic surfaces are known to be less prone to fouling. Ultrafiltration membranes are frequently prepared from rather hydrophobic polymers like polysulfone (PSU). Strategies to keep the good pore forming characteristics of PSU, but with improved hydrophilicity are proposed here. PSU functionalized with 1,2,3-triazole ring substituents containing OH groups was successfully synthesized through click chemistry reaction. The structures of the polymers were confirmed using NMR spectroscopy and Fourier transform infrared spectroscopy (FTIR). High thermal stability (>280°C) was observed by thermal gravimetric analysis. Elemental analysis showed the presence of nitrogen containing triazole group with different degrees of functionalization (23%, 49%, 56%, and 94%). The glass transition temperature shifted with the introduction of triazole pendant groups from 190°C (unmodified) to 171°C. Ultrafiltration membranes were prepared via phase inversion by immersion in different coagulation baths (NMP/water mixtures with volume ratios from 0/100 to 40/60). The morphologies of these membranes were studied by field emission scanning electron microscopy (FESEM). The optimized PSU bearing triazole functions membranes exhibited water permeability up to 187 L m^{-2} h^{-1} bar^{-1}, which is 23 times higher than those prepared under the same conditions but with unmodified polysulfone (PSU; 8 L m^{-2} h^{-1} bar^{-1}). Results of bovine serum albumin protein rejection test indicated that susceptibility to fouling decreased with the modification, due to the increased hydrophilicity, while keeping high protein rejection ratio (>99%). © 2014 Wiley Periodicals, Inc. J. Appl. Polym. Sci. **2015**, *132*, 41549.

KEYWORDS: functionalization of polymers; membranes; separation techniques; synthesis and processing

Received 17 July 2014; accepted 10 September 2014
DOI: 10.1002/app.41549

INTRODUCTION

Membrane separation technology offers great promises to meet the more stringent regulatory requirements for water quality that cannot be easily reached by conventional treatment technologies. Needed separation membranes are strong, thermally stable, and resistant to oxidative or corrosive elements in the material to be separated such as acids or chloride ions.[1] PSU is one of the high-performance polymer family widely used for fabrication of membranes. The developments of PSU membranes can be traced in the 1960s as an alternative to cellulosic membranes. A great advantage over cellulose acetate in terms of membrane applications is its resistance in extreme pH conditions and chlorinated disinfectants. Other excellent properties of PSU include good mechanical roughness, hydrolytic stability, as well as thermal stability with a T_g of 190°C.[2,3] PSU is soluble in many solvents, so can be easily applied in conventional phase separation processes with good pore forming behavior.[2] Due to these properties, PSUs have been the basis of several applications, such as microfiltration membranes,[4] electrospun nanofibrous scaffold for thin film composite nanofiltration membranes,[5] mixed matrix membranes for gas separation,[6] proton exchange membranes for fuel cell,[7] and capillary fiber as a drug delivery device for intraocular applications.[8]

However, a drawback for the application of PSUs membranes for aqueous phase is their intrinsic hydrophobicity[9,10] which causes fouling. To overcome this limitation, a good strategy for improving fouling resistance is the introduction of hydrophilic functionalities groups covalently bonded to the PSUs backbone[11–13] or surface of polymer membranes.[10,13,14] Modified membranes are expected to have low adsorption of hydrophobic materials such as protein and other solutes.[11,15–19] It should affect the membrane processes such as reverse osmosis, nanofiltration, and ultrafiltration. It is also expected to control hydrophobic and hydrophilic nature within the membrane physical structure and enhances the transport properties.[10,15,16] Introduction of functionality to PSUs can be accomplished by either using the functional monomer approach allowing modification at the polymerization stage (polycondensation) or by the post-functionalization of commercially available polymers.[2]

Introduced by Sharpless and coworkers,[20] the click chemistry concept enables the preparation of not only telechelic polymers

Additional Supporting Information may be found in the online version of this article.

but also side-group functionalized polymers using clickable initiators, monomers or polymers in nearly quantitative yields.[21–23] The click reaction is also well known for the broad tolerance toward functional groups, low susceptibility to side reactions allowing mild reaction conditions and easy isolation of final products.[20] Owing to these merits click chemistry has been demonstrated as a powerful tool for the grafting modification of polymer materials.[24,25] Our approach in the present work, is to modify PSU in different degree of functionalization (DF) by using a well-known click reaction, the copper(I)-catalyzed azide-alkyne cycloaddition (CuAAC) between an organic azide and a terminal alkyne.[20–23] Recently Dimitrov *et al.*[26,27] grafted phosphonated poly(pentafluorostyrene) onto PSU backbone via the click chemistry approach to improve proton conductivity of dense membranes for fuel cell. In their work lithiation chemistry was employed to introduce 3-(chloromethyl)benzoyl pendent groups on PSU that was subsequently converted to the clickable 3-(azidomethyl)benzoyl groups. In this study PSU was first chloromethylated on phenyl rings and finally yielded a stable 1,4-disubstituted 1,2,3-triazole ring having OH substituent through CuAAC. Using the modified PSU, we prepared ultrafiltration membranes and studied their morphologies and performance, and the effect of coagulation bath composition.

EXPERIMENTAL

Materials

PSU (Sigma Aldrich) was dried overnight at 110°C in vacuum oven prior to use. Copper (I) bromide (CuBr, 98%, Sigma Aldrich) was purified overnight by reflux in acetic acid (glacial, Fisher Scientific), then filtering and washing solids five times with absolute ethanol (≥99.5%, Sigma Aldrich) and ten times with diethyl ether (≥99.5%, Carl Roth). It was then dried under vacuum to remove any residual solvents.[28] Activated aluminum oxide (Al_2O_3, basic, Brockman I, Sigma Aldrich), *N*,*N*,*N*′,*N*″,*N*″-Pentamethyldiethylenetriamine (PMDETA, 99%; Sigma Aldrich), Tin(IV) chloride ($SnCl_4$, 99%; Sigma Aldrich), chlorotrimethylsilane (≥99%; Sigma Aldrich), paraformaldehyde [$(CH_2O)_n$, 95%; Sigma Aldrich], sodium azide (NaN_3, ≥99.5%; Sigma Aldrich), propargyl alcohol (99%; Sigma Aldrich), ammonium in solution (volumetric, ~1% NH_3, ~2% Cl^- in H_2O; Sigma Aldrich), chloroform ($CHCl_3$, 99+%; Fisher Scientific), *N*,*N*-dimethylformamide (DMF, ≥99.5%; Carl Roth), tetrahydrofuran (THF, ≥99.5%; Carl Roth), methanol (≥99%; Fisher Scientific), and *N*-methylpyrrolidinone (NMP, ≥99.5%; Sigma Aldrich) were used as received. Deoxygenation was achieved by bubbling nitrogen through the material for approximately 45 min before it was introduced into the flask.

Characterization

^1H and ^{13}C NMR spectra were recorded with a Bruker AVANCE-III spectrometer at a frequency of 500 MHz using a cryo probe at room temperature and deuterated solvents with tetramethylsilane $Si(CH_3)_4$ as an internal standard.

The polymer's molar mass and its distribution were determined by tetra detection gel permeation chromatography (GPC) from Viscotek using a GPCmax module (model VE-2001) and a GPC-TDA 305 system equipped with two columns (LT4000L, Mixed, Low Org. 300 mm × 8.0 mm) eluted at 1.0 mL min^{-1} in stabilized THF eluent at 35°C and with four detectors: UV, light scattering (RALS and LALS), refractive index, and viscometer. Absolute molecular weights were determined using polystyrene standards for calibration. Samples were stirred for 12 h in stabilized THF and then, passed through a 25 mm × 0.45 μm teflon filter before measurement.

Fourier transform infrared-attenuated total reflectance (FTIR-ATR) spectra were recorded at room temperature on a Perkin-Elmer 100 equipped with a universal ATR. Solid membrane was placed over the ATR crystal and maximum pressure was applied using the slip-clutch mechanism. Data were collected over 16 scans with a resolution of 4 cm^{-1}.

Elemental analysis was made on a Perkin Elmer 2400 Series II, CHNS/O Analyzer equipped with AD6 Autobalance Controller.

Thermogravimetric analysis (TGA) was conducted using a TGA Q50 (TA instruments) with a heating rate of 10°C min^{-1} under nitrogen flow from 30 to 800°C. Differential scanning calorimetry (DSC) was carried out on a Perkin-Elmer DSC 204 F1 NETZSCH under nitrogen flow. The heating rate was 10°C min^{-1} and the cooling rate was 5°C min^{-1} in the range of temperature from 25 to 220°C. The samples were placed in aluminum pans and heated from 25 to 220°C under a nitrogen flow rate. The glass transition temperature (T_g) of each sample was taken from the second heating scan.

Contact angle measurement was performed on a Krüss Easydrop equipment in static mode at ambient temperature. Membranes formed in pure water coagulation bath were used to investigate the hydrophilicity of corresponding polymers. Each contact angle was reported as the average from three measurements.

The surface and cross section morphology of the membranes were observed by FESEM in a FEI Quanta 200 FEG SEM. For surface imaging, a small piece of membrane sample was mounted on a flat aluminum stub, fixed by aluminum conductive tapes. For cross section, the membrane sample was freeze-fractured in liquid nitrogen, and mounted on a 90° aluminum stub vertically with double-coated carbon tapes. The samples were sputter-coated with Au/Pd for 20 s at 20 mA to prevent electron charging using a K575X Emitech equipment. All the images were taken using a secondary electrons detector, at 5 kV, 16 pA and working distance of 5 mm. Images were obtained at different magnifications. Each sample was imaged at more than five locations to ensure the reproducibility of the features observed.

Capillary flow porometry was measured in POROLUX™ 1000 porometer to obtain the pore size distribution of membranes. Porefill (16 mN m^{-1}) was used as the wetting liquid, which was displaced by nitrogen gas flow with the pressure up to 34.5 bar.

Synthesis of Chloromethylated PSU (PSU-CH_2Cl)

Chloromethylation was performed following similar procedures reported by Avram *et al.*[29]

PSU (22 g, corresponding to 49.71 mmol of repeating unit) was dissolved in 750 mL of $CHCl_3$ (2 wt % PSU) in a 1-L three-necked round bottom flask with a stir bar equipped with a reflux condenser under nitrogen atmosphere for 1 h. Paraformaldehyde (15 g, 499.5 mmol) was added to the flask and the

solution was mixed while raising the temperature to 52°C; At 52°C, chlorotrimethylsilane (63 mL, 497.14 mmol) and $SnCl_4$ (0.22 mL, 1.91 mmol) as catalyst were added. The headspace of the condenser was blanketed with nitrogen and sealed. The reaction was carried out at different times (24, 48, 72, and 84 h), respectively, to give rise to different DF. At the end of the experiment, the reaction mixture was filtered. The filtrate was concentrated and precipitated in methanol. The polymer was subsequently dissolved in chloroform and reprecipitated in methanol, then filtered and dried under vacuum overnight at 60°C yielding white amorphous solid, soluble in common organic solvents. Yield: 20 g (91%). They are named with the DF as PSU-$CH_2Cl_{0.23}$, PSU-$CH_2Cl_{0.49}$, PSU-$CH_2Cl_{0.56}$, and PSU-$CH_2Cl_{0.94}$.

PSU-$CH_2Cl_{0.23}$: ^{1}H NMR (500 MHz, 298K, $CDCl_3$, ppm) δ: 7.89–7.82 (m, 4H, e protons), 7.36 (d, 1H, g proton), 7.24 (d, 2H, b protons), 7.16 (dd, 1H, b′ protons), 7.05–6.97 (m, 4H, d protons), 6.94 (m, 2H, a protons) and 6.84 (m, 2H, a′ protons), 4.53 (m, 2H, f protons), and 1.7 (m, 6H, c protons).

PSU-$CH_2Cl_{0.23}$: ^{13}C NMR (500 MHz, 298K, $CDCl_3$, ppm) δ: 162.21–161.98 (C_{21}), 161.70 (C_{14}), 153.0–152.81 (C_1 and C_{13}), 151.08 (C_{13}), 147.86 (C_7), 146.86 (C_4), 147.28 ($C_{7'}$), 135.96 (C_{17}), 135.53–135.37 (C_{17} and C_{18}), 135.28 ($C_{17'}$), 129.97–129.68 (C_{16} and C_{20}), 129.56 (C_{10}), 129.11(C_{11}), 128.57 (C_3 and C_8), 120.28–119.84 (C_2 and C_9), 118.01–117.63 (C_{15} and C_{19}), 42.63–42.44 (C_5), 41.11 (C_{12}), and 31.13–30.93 (C_6).

Synthesis of Azidomethyl Polysulfone (PSU-CH_2N_3)

Azidation was conducted with sodium azide in DMF.[30,31]

PSU-CH_2Cl (10 g, 8.14 mmol chloromethyl group per repeat unit; 72 h) was dissolved in 200 mL of DMF in a two-necked round bottom flask. Sodium azide (1.66 g, 24.45 mmol) was added to the solution. The mixture was stirred at 60°C under nitrogen for 24 h. At the end of the experiment, the resulting product was precipitated into a mixture of methanol and water (4 : 1, v : v) and washed three time with water to remove the excess of sodium azide. After filtration, the obtained polymer (PSU-CH_2N_3) was dissolved in chloroform and reprecipitated in methanol, then filtered and dried under vacuum for 24 h at 60°C. Yield: 9 g (90%).

PSU-$CH_2N_{3;0.23}$: ^{1}H NMR (500 MHz, 298K, $CDCl_3$, ppm) δ: 7.90–7.82 (m, 4H, e protons), 7.24 (m, 2H, b protons), 7.20 (m, 1H, b′ protons), 7.05–6.97 (m, 4H, d protons), 6.94 (m, 2H, a protons) and 6.88 (m, 2H, a′ protons), 4.28 (m, 2H, f′ protons), and 1.7 (m, 6H, c protons).

PSU-$CH_2N_{3;0.23}$: ^{13}C NMR (500 MHz, 298K, $CDCl_3$, ppm) δ: 162.21–161.98 (C_{21}), 161.70 (C_{14}), 153.0–152.81 (C_1 and C_{13}), 151.08 (C_{13}), 147.86 (C_7), 146.86 (C_4), 147.28 ($C_{7'}$), 135.96 (C_{17}), 135.53–135.37 (C_{17} and C_{18}), 135.28 ($C_{17'}$), 129.97–129.68 (C_{16} and C_{20}), 129.56 (C_{10}), 129.11(C_{11}), 128.57 (C_3 and C_8), 120.28–119.84 (C_2 and C_9), 118.01–117.63 (C_{15} and C_{19}), 49.86 ($C_{12'}$), 42.61–42.45 (C_5), and 31.23–30.55 (C_6).

Click-Chemistry of Azidomethyl Polysulfone (PSU-TrN)

In order to prepare PSU bearing 1,2,3-triazole functions; PSU-CH_2N_3 [7.0 g, 3.52 mmol of azidomethyl group, 1 equivalent; DF = 0.23] was dissolved in DMF (140 mL) in a round bottom schlenk flask sealed with a rubber septum. Next, degassed PMDETA (2.20 mL, 10.56 mmol, 3 equivalents) and propargyl alcohol (0.22 mL, 3.87 mmol, 1.1 equivalents) was added to the flask via syringe under nitrogen. The mixture was degassed by one freeze-pump-thaw cycle. Then CuBr (1.5148 g, 10.56 mmol, 3 equivalents) was added quickly in the frozen state. Immediately after that, the flask was subjected to five additional freeze–pump–thaw cycles to remove oxygen. Finally, the flask was placed in a constant-temperature oil bath at 60°C and stirred for 24 h. After the reaction was terminated by exposure to air and cooled down to room temperature, the solution was then poured into 3 L of 0.5% aqueous ammonia solution to remove majority of copper complex. The polymer was solubilized into a large amount of THF and filtered through a column of activated basic Al_2O_3. The filtrate was concentrated under reduced pressure and then, precipitated in an excess of methanol. The purified polymer was dried in vacuum oven at 60°C for 24 h. The same procedure was carried out to synthesize PSU-$TrN_{0.49}$, PSU-$TrN_{0.56}$, and PSU-$TrN_{0.94}$, except that for PSU-$TrN_{0.94}$ the polymer was solubilized in DMF instead of THF in the purification stage.

PSU-$TrN_{0.23}$: ^{1}H NMR (500 MHz, 298K, DMSO-d_6, ppm) δ: 7.94–7.79 (m, 4H, e proton), 7.78 (m, 1H, g proton), 7.32 (m, 1H, i proton), 7.29–7.10 (m, 3H, b, b′ proton), 7.10–6.81 (m, 8H, d, a, a′ proton), 5.45 (m, 2H, h proton), 5.11 (m, 1H, k proton), 4.31 (m, 2H, j proton), and 1.58 (m, 6H, c protons).

PSU-$TrN_{0.23}$: ^{13}C NMR (500 MHz, 298K, DMSO-d_6, ppm) δ: 162.21–161.98 (C_{21}), 161.70 (C_{14}), 153.0–152.81 (C_1 and C_{13}), 151.08 (C_{13}), 147.86 (C_7), 146.86 (C_4), 147.28 ($C_{7'}$), 135.96 (C_{17}), 135.53–135.37 (C_{17} and C_{18}), 135.28 ($C_{17'}$), 129.97–129.68 (C_{16} and C_{20}), 129.56 (C_{10}), 129.11(C_{11}), 128.57 (C_3 and C_8), 120.28–119.84 (C_2 and C_9), 118.01–117.63 (C_{15} and C_{19}), 54.91 (C_{25}), 48.24 (C_{22}), 41.93 (C_5), and 30.49 (C_6).

The numbering of ^{1}H and ^{13}C for NMR chemical shifts can be found in Figure S1 (Supporting Information).

Preparation of PSU-TrN Membranes

All the membranes in this work were prepared via a typical non-solvent induced phase separation (NIPS) method.[32,33] The casting solution from 18 wt % Polymer-NMP was stirred for 12 h to obtain a homogeneous solution. The solution was sonicated for 15 min and kept still for 12 h to release bubbles. The viscous solution was cast onto a clean glass plate with a 200-μm high casting knife. The plate was then immersed quickly and smoothly into the coagulation bath with varying water/solvent ratio by weight at room temperature. After a period of time (3–5 min) in the primary coagulation bath, the plate was removed and the membrane was placed in a deionized water bath for exhaustive extraction of solvent during 12 h before the experiment. The resulting opaque porous films had an average thickness of 100 μm.

Ultrafiltration Experiments

Ultrafiltration experiments were conducted using a dead-end magnetically stirred Amicon cell with an effective membrane area of 4.1 cm^2 to evaluate the membranes performance. The membrane was precompacted by deionized water for 1 h at operation pressure of 2 bars and the stable pure water

permeance was recorded denoted as J_{w1}. The permeance was calculated by using the following equation:

$$J = \frac{V}{tS\Delta P} \quad (1)$$

where V and t are the volume of the permeate and the time to collect it, respectively; S is the effective membrane area; ΔP is the transmembrane pressure. Afterward, the feed solution was replaced by 1 mg mL^{-1} of bovine serum albumin solution to conduct protein filtration test for 1 h. The permeance of protein filtration was measured as J_p. The γ-globulin rejection ratio R was calculated according to the following equation:

$$R = \left(1 - \frac{C_p}{C_b}\right) \times 100\% \quad (2)$$

where C_p and C_b are the bovine serum albumin concentrations of the permeate solution and bulk solution in the feed side, respectively. The concentration was determined by a UV–Vis spectrophotometer (Shimadzu, UV 2550) at 278 nm. Then the membrane was vigorously flushed by deionized water for 10 min. Subsequently, pure water permeance of the cleaned membrane was measured again as J_{w2} in the same manner.

RESULTS AND DISCUSSION

Functionalization of PSU

As depicted in Scheme 1, the first step of the modification was the chloromethylation of PSU polymer [Scheme 1(a)], following a procedure analogous to that described by Avram *et al.*[29] The precursor chloromethylating reagent was formed in chloroform from paraformaldehyde, chlorotrimethylsilane, and $SnCl_4$ as a catalyst. The overall molar ratio of polymer to reagents was 1 : 10 : 10 and with PSU concentration in $CHC1_3$ of 2%. The reaction proceeded at 50°C until the desired DF was achieved. Four polymers (PSU-CH_2Cl_i, with i = DF) were synthesized at different experiment times such as 24, 48, 72, and 84 h leading to DF of 23, 49, 56, and 94 mol %, respectively. The yields of the corresponding random copolymers were up to 92 wt %. It is important to note that the soluble chloromethylated PSUs (PSU-CH_2Cl) can be obtained only when the chloromethylation is performed at the high dilution and low catalyst amounts. The increase in the reaction time or reagent concentration degrades the polymer. The chloromethyl side groups of PSU-CH_2Cl were reacted with sodium azide in DMF at 60°C. Thus, PSU was quantitatively converted into a backbone carrying "clickable" azide side groups, PSU-CH_2N_3[30,31] [Scheme 1(b)].

Finally, the click chemistry reaction was performed by using PSU-CH_2N_3 and propargyl alcohol to obtain good yield of modified PSU bearing 1,2,3-triazole groups [PSU-TrN; Scheme 1(c)].[2,30,31] In each step of synthesis the resulting polymer was recovered with more than 90% yield. All these steps were characterized by NMR (^1H and ^{13}C) spectroscopy to confirm the polymer structure. Typical ^1H NMR spectra are given in Figure 1 for unmodified PSU, PSU-$CH_2Cl_{0.23}$, PSU-$CH_2N_{3;0.23}$, and PSU-$TrN_{0.23}$ obtained after a reaction time of 24 h during chloromethylation step. As seen in the spectra, the chemical shifts at δ = 6.80–7.95 ppm are assigned to the protons of phenyl rings of the PSU backbone. For the resonance at δ = 4.53

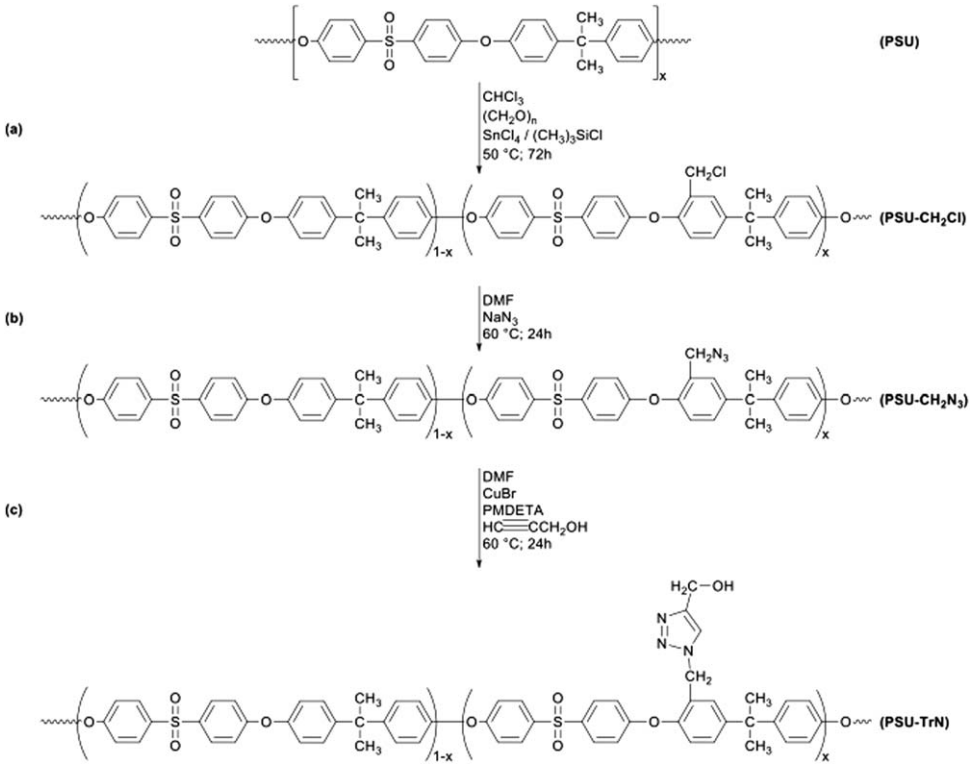

Scheme 1. Schematic representation of the synthetic route to functionalized polysulfone (PSU). Synthesis of (a) chloromethylated polysulfone (PSU-CH_2Cl), (b) azidomethylated polysulfone (PSU-CH_2N_3), and (c) formation of polysulfone bearing 1,2,3-triazole groups by click reaction.

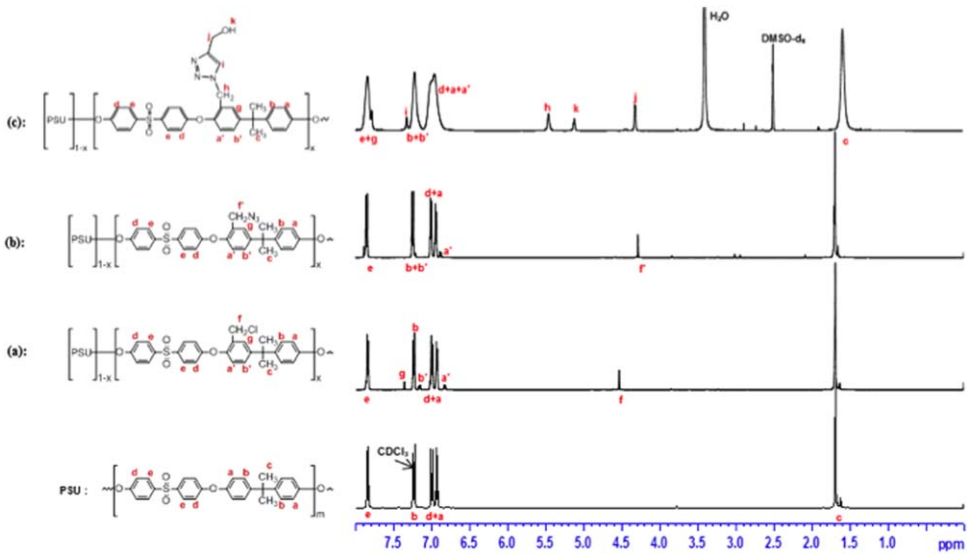

Figure 1. ^{1}H NMR for PSU, PSU-$CH_2Cl_{0.23}$, PSU-$CH_2N_{3;0.23}$ recorded in $CDCl_3$ and PSU-$TrN_{0.23}$ recorded in DMSO-d5. [Color figure can be viewed in the online issue, which is available at wileyonlinelibrary.com.]

ppm [Figure 1(a)], it can be assigned to the methylene protons of the repeating unit of PSU-CH_2Cl (i.e., –C**H**$_2$–Cl). Subsequently, after the substitution reaction, the resonance for the CH_2Cl protons at 4.53 ppm completely disappeared in the NMR spectrum of the product whereas a new resonance at 4.28 ppm [Figure 1(b)] with the same intensity corresponding to the methylene protons of the repeating unit of PSU-CH_2N_3 (i.e., –C**H**$_2N_3$) appeared. Furthermore, not only there was no apparent change in the polydispersity of the PSU-CH_2N_3 compared to the precursor PSU-CH_2Cl according to SEC analysis (Figure 2; i.e., DF = 0.56), but PSU-CH_2N_3 displayed the characteristic stretching band of $-N_3$ which appeared at 2100 cm^{-1} in the FTIR spectrum [Figure 3(c)]. The "click" chemistry approach was performed in the presence of CuBr/PMDETA in DMF at 60°C and was also shown to proceed in quantitative yields as the absorption band of azide at 2100 cm^{-1} disappeared in the FTIR spectrum [Figure 3(d)], suggesting complete functionalization. A new and broad band at 3150–3770 cm^{-1} also appeared due to the stretching vibration of O–H groups[34] linked to the triazole ring. Moreover, a resonance at 5.45 ppm corresponding to the methylene protons linking the phenyl ring and the triazole ring in the side chains was clearly visible in the NMR spectrum of the product [Figure 1(c)]. In addition, we can also observe the emergence of three new peaks: A resonance at 5.11 ppm assigned to the proton of the hydroxyl group, a resonance at 4.31 ppm assigned to the methylene protons located in the alpha position of the hydroxyl group and the resonance at 7.32 ppm assigned to the proton of the triazole ring.

^{1}H NMR and elemental analysis (Table I) easily quantitates the DF of the product materials for PSU-CH_2Cl and PSU-CH_2N_3. From elemental analysis, the DF was determined from the nitrogen content of PSU-CH_2N_3, and varies with different chloromethylation time from 24 to 84 h. On the other hand from ^{1}H NMR, DF can be estimated from the integration ratio of the $-CH_2$ protons from the chloromethyl protons of the side groups at $\delta = 4.53$ to the integrals of the signals at 7.95–7.80 ppm of the four meta protons (e protons, Figure 1) of the phenyl ring adjacent to the sulfonyl group. The molecular weights of the obtained polymers are listed in Table I. In principle, there should be no large deviation of the Mn of these polymers since only small units (–Cl, $-N_3$, and triazole) were attached to the same backbone. For polymers with the highest DF, exceptionally high values for M_n and I_p were detected. We believe that the anomalous value for PSU-CH2Cl0.94 and PSU-N3;0.94 could be attributed to the formation of intermolecular methylene bridges during the chloromethylation,[2] under the high DF (94%). From Figure 3, the absorption bands at 1293, 1150 and 1082 cm^{-1} are assigned to the symmetric and asymmetric stretching vibrations of –S=O present in backbone of polymer chains.[34,35] The absorption bands at 2966 and 2924 cm^{-1} are attributed to the aromatic and aliphatic stretching vibrations of $-CH_2$ groups. The peaks at 1579 and 1483 cm^{-1} are assigned to

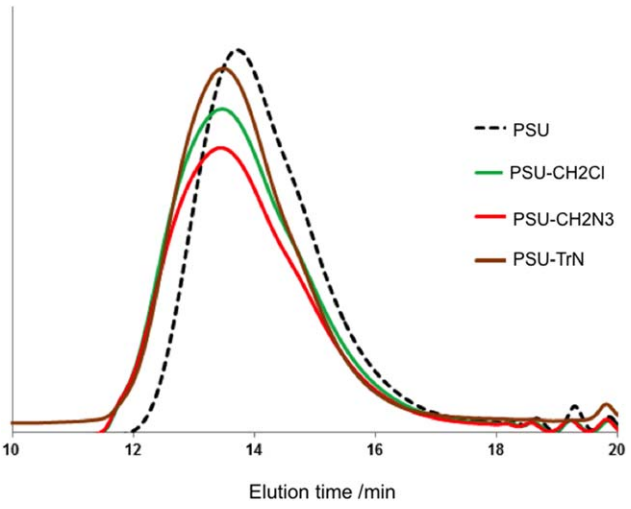

Figure 2. GPC traces for PSU, PSU-$CH_2Cl_{0.56}$, PSU-$CH_2N_{3;0.56}$ and PSU-$TrN_{0.56}$. [Color figure can be viewed in the online issue, which is available at wileyonlinelibrary.com.]

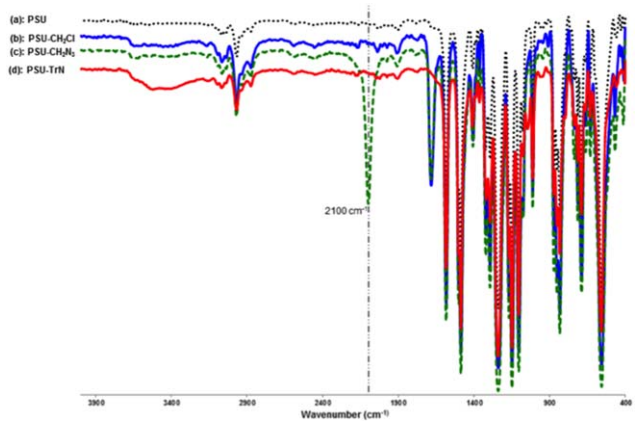

Figure 3. FTIR spectra for (a) unmodified PSU, (b) PSU-$CH_2Cl_{0.94}$, (c) PSU-$CH_2N_{3;0.94}$, and (d) PSU-$TrN_{0.94}$. [Color figure can be viewed in the online issue, which is available at wileyonlinelibrary.com.]

the stretching vibration of aromatic hydrocarbons. The absorption band at 1232 cm^{-1} is ascribed to asymmetric vibration of the ether linkage.

Thermal Properties

The thermal properties of the functionalized copolymers as well as those of the precursor PSU were evaluated by their thermal decomposition and glass transition data as listed in Table II. Figure 4 shows the TGA curves of the precursor and modified PSU wherein a three-step weight loss was observed in all the modified polymers. The first and lower loss appeared in the range of 250 to 366°C, 175 to 275°C, and 241 to 416°C, respectively, for PSU-CH_2Cl, PSU-CH_2N_3, and PSU-TrN, was presumably due to the elimination of the functional unit. The main decomposition occurs in the second or third steps[36] and was related to the degradation of the polymer backbone. At $T_{d5\%}$, the chemical modification reaction and subsequent substitution reaction of chlorine with azide and 1,2,3-triazole derivatives led to a significant decrease in the thermal stability of PSU.[36] It is also observed that the thermal stability of chloromethylated and azido polymers decreases with the increase in the DF.

Table I. Characteristics of the Synthesized Polymers

Sample	DF[a]	DF[b]	M_n (g mol^{-1})[c]	I_p
PSU-$CH_2Cl_{0.23}$	0.23	—	39,300	1.93
PSU-$CH_2Cl_{0.49}$	0.49	—	44,900	2.03
PSU-$CH_2Cl_{0.56}$	0.56	—	44,300	2.22
PSU-$CH_2Cl_{0.94}$	0.94	—	58,700	3.80
PSU-$N_{3;0.23}$	0.26	0.25	39,500	1.93
PSU-$N_{3;0.49}$	0.49	0.44	42,800	2.17
PSU-$N_{3;0.56}$	0.56	0.55	43,100	2.30
PSU-$N_{3;0.94}$	0.96	0.92	60,800	3.67

[a] Degree of functionalization per repeating unit determined by ^1H NMR.
[b] Degree of functionalization determined from elemental composition of nitrogen.
[c] Determined by GPC with PS standards.

Table II. Polymers Thermal Properties

Sample	T_g (°C)	$T_{d5\%}$ (°C)	$T_{d10\%}$ (°C)
PSU	190	460	467
PSU-$CH_2Cl_{0.23}$	192	399	442
PSU-$CH_2Cl_{0.49}$	184	333	397
PSU-$CH_2Cl_{0.56}$	193	325	392
PSU-$CH_2Cl_{0.94}$	179	320	392
PSU-$CH_2N_{3;0.23}$	199	401	426
PSU-$CH_2N_{3;0.49}$	208	366	403
PSU-$CH_2N_{3;0.56}$	210	363	405
PSU-$CH_2N_{3;0.94}$	203	305	380
PSU-$TrN_{0.23}$	183	376	418
PSU-$TrN_{0.49}$	179	330	380
PSU-$TrN_{0.56}$	178	342	376
PSU-$TrN_{0.94}$	170	387	420

As expected from the DSC measurements, we observed for the triazole functionalized polymers that the increase in the DF led to a decrease in T_g. The T_g of the PSU (190°C) decreased gradually to 183°C for PSU-$TrN_{0.23}$ and 170°C for PSU-$TrN_{0.94}$ (Table II; Figure 5). The triazole-OH side groups might act as spacers, creating more space between the PSU chains. This disfavors the strong interaction between polar SO_2 groups from different chains, as observed before by Gaina *et al.*[30] for chloromethylated PSUs. Furthermore the functionalization is random, affecting the regularity of the repeating units and again disturbing, intermolecular packing. As a result the functionalization decreases T_g.

Membrane Preparation

All the polymers were readily soluble in polar aprotic solvents such as DMSO, DMF, DMAc, and NMP. The membranes in this work were all fabricated by solution casting and phase inversion method.[32,33] All membranes were very robust, easy to

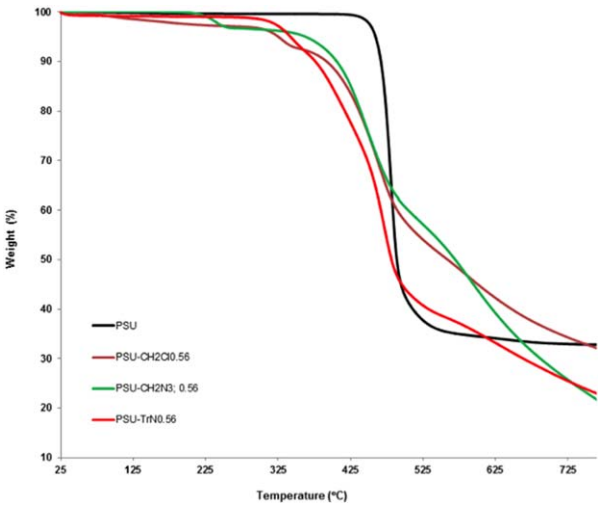

Figure 4. TGA curves for PSU, PSU-$CH_2Cl_{0.56}$, PSU$CH_2N_{3;0.56}$, and PSU-$TrN_{0.56}$. [Color figure can be viewed in the online issue, which is available at wileyonlinelibrary.com.]

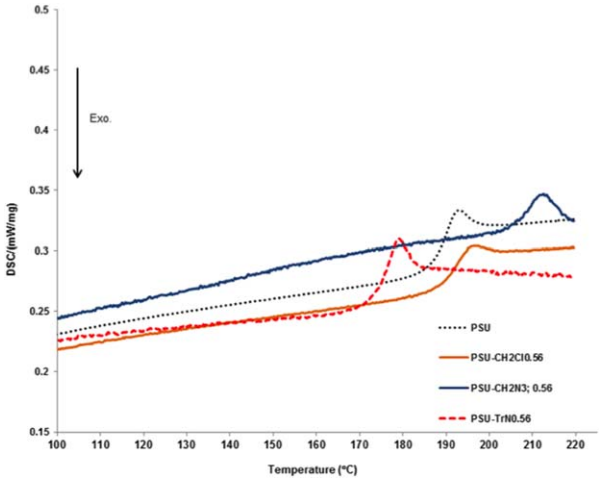

Figure 5. DSC curves for PSU, PSU-$CH_2Cl_{0.56}$, PSU$CH_2N_{3;0.56}$, and PSU-$TrN_{0.56}$. [Color figure can be viewed in the online issue, which is available at wileyonlinelibrary.com.]

handle and had good film forming properties. The compositions of the casting solution and coagulation bath were shown in Table III.

Hydrophilicity of the Membranes

Membranes' hydrophilicity was evaluated with contact angle measurements using deionized water on all membranes. The observed contact angles are presented in Table III. As expected, the contact angle of the plain PSU membrane was high (81°), confirming the hydrophobic nature. The contact angle monotonously decreased with increase in the DF of the membrane, indicating that the functionalization effectively increased the hydrophilicity of PSU membranes. The lowest contact angle (70°) was obtained for membrane cast from PSU-$TrN_{0.94}$. This is due to the attachment of hydrophilic group (1*H*-1,2,3-triazol-4-yl) on the PSU backbone and responsible for the formation of tight hydration layer on the membrane surface through hydrogen bonding with water molecules.

Table III. Permeability and Contact Angle of Membranes Prepared From 18 wt % Polymer Casting Solutions in NMP, With Different Coagulation Baths

Polymer	Coagulation bath (v/v %)	Contact angle (°)	Permeability (L m^{-2} h^{-1} bar^{-1})
PSU	100 H_2O	80.7 ± 2.5	7.6 ± 3.9
	40 H_2O, 60 NMP	—	0
PSU-$TrN_{0.23}$	100 H_2O	77.0 ± 0.2	18.6 ± 3.0
	40 H_2O, 60 NMP	—	5.4 ± 3.4
PSU-$TrN_{0.49}$	100 H_2O	74.5 ± 1.3	55.4 ± 18.6
	40 H_2O, 60 NMP	—	52.3 ± 1.2
PSU-$TrN_{0.56}$	100 H_2O	71.2 ± 1.5	121.6 ± 66.4
	40 H_2O, 60 NMP	—	46.8 ± 3.9
PSU-$TrN_{0.94}$	100 H_2O	70.0 ± 2.0	187.0 ± 56.5
	40 H_2O, 60 NMP	—	72.0 ± 28.8

Morphology of Membranes

The membrane surface and the cross-section FESEM images are shown in Figures 6 and 7. A surface image for a membrane prepared from PSU-$TrN_{0.49}$ membrane is shown in Figure 6. Similar morphology was observed for the surface of other membranes prepared with different DFs are similar, indicating similar pore size and pore density. As confirmed by the cross-section images, all membranes obtained by coagulation in water bath exhibited a typical asymmetric structure with finger-like macrovoids.[37] The formation of the large macrovoids is due to fast exchange rate between solvent and nonsolvent during the membrane preparation.[37,38] Figure 7 shows that when solvent (NMP) is added to the coagulation bath the surface porous structure changes. The surface porosity decreases and pores are more heterogeneous as macropores are formed among the smaller pores. Although finger-like cavities are still present in membranes coagulated in a mixture of water and NMP, a sponge-like structure co-occurs and predominates for polymers with higher DF. The use of NMP/H_2O (60/40) in coagulation bath slows the phase inversion kinetics. The driving force for solvent–non solvent exchange between polymer solution and NMP/H_2O nonsolvent bath is smaller (smaller osmotic pressure), the top skin is slowly formed as well as the sub layer leading to the more homogeneous sponge structure. When the coagulation bath has only water, the membrane skin is formed fast, while still a large amount of solvent is still present in the sublayer. The driving force for solvent-nonsolvent exchange is large. Water penetrates the polymer solution layer preferentially in weaker points (interfacial tension inhomogeneities) of the incipient skin and finger like cavities are formed. When very hydrophobic polymers are used for the "phase inversion" membrane manufacture, the penetration of small amount of water is enough to induce immediate polymer coagulation. A thin and dense skin is formed along the path of water penetration resulting in the finger-like cavities of most hydrophobic membranes in Figure 6. For hydrophilic polymers the homogeneous part of the water-NMP-polymer phase diagram is expected to be larger. Even with larger amount of water, the solution might not phase-separate, since the hydrophilic OH groups improves the thermodynamic interaction between polymer and water-solvent mixture. Phase separation will start only, when water-solvent exchange proceeds to a larger extent than in the case of unmodified PSU. Water-solvent exchange also leads to gelation. The morphology induced by phase separation will evolve until gelation reduces the mobility of the polymer-rich phase enough to "freeze" the system. The sizes of pores and the porous structure depend on how far the starting condition for phase separation is from gelation. This explains the differences in morphology observed for different DFs.

Permeability

Water fluxes were measured and the results are depicted in Figure 8 and Table III. The water flux values increased proportionally to the increase in the DF: 8, 55, 122, and 187 L m^{-2} h^{-1} bar^{-1}, respectively, for DFs 23, 49, 56, and 94 mol %. These results can also be associated with the increase in the hydrophilicity (contact angle) observed in Table III. The improved hydrophilicity enhances the water permeability by

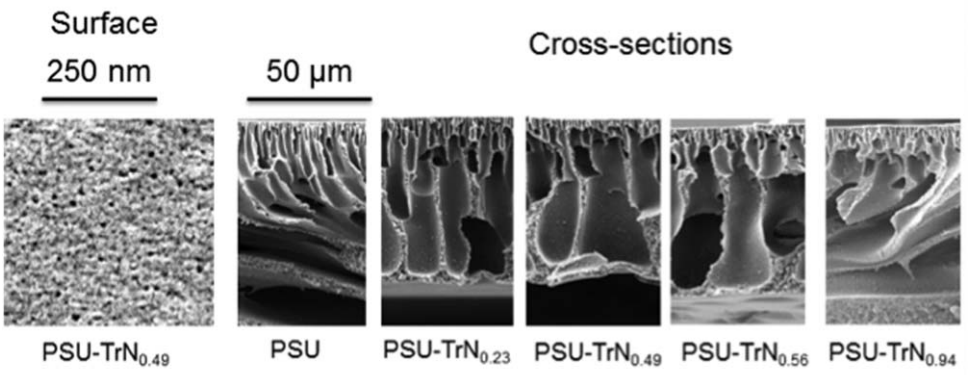

Figure 6. Morphology of surfaces and cross sections of membranes prepared by phase inversion in water.

facilitating wetting and transport through the membrane. Moreover, the pores size and their interconnectivity at least as relevant for the membrane permeability as the hydrophilicity, as well as the thickness of the most selective layer or top region with smallest pores, contributing most to the flux resistance.

The pores imaged on the membranes surfaces do not change much, although the most hydrophilic membranes coagulated in NMP/H_2O seem to be larger. For the same polymer, the pure water permeability of membranes prepared in NMP/H_2O coagulation bath is lower than that of membranes prepared in water. It is proposed that the sponge like structures obtained in NMP/H_2O probably contains closed cells, which are not accessible for water transport in the final membrane. The lack of interconnectivity is indicated by the pore size distribution obtained from a gas-liquid displacement capillary flow porometer. As shown in Figure 9, the diameter of most of the pores inside the membranes is measured to be around 100 nm. This value is far smaller than the pore size observed from SEM images of membrane surfaces. The absence of large surface pores in the porometry suggests that these pores are either "dead", completely closed by the cells that are not interconnected, or limited by the smaller openings between the cells in the sponge-like sublayer. Thus they are unable to contribute to the water permeation.

Protein Retention and Fouling

The membranes' selectivity for bovine albumin, which has a molecular weight of 69 kg mol^{-1} was evaluated. The retention is higher than 99% for all membranes. If permeability and separation factors are plotted for the different membranes together with values for other PSU membranes reported in the literature, similar to the plot published by Mehta and Zydney,[39] as shown in Figure 10. Our membranes are characterized by very high separation factors, compared to other available membranes. The most hydrophilic membranes are on the front limit of the trend curve, while the hydrophobic membranes are far from the curve. The literature values depicted in Figure 10 include PSU and the more hydrophilic polyethersulfone membranes, without distinguishing them, also without specifying molecular weight, membrane preparation conditions and presence of additives. The plot however gives us a rough indication on how the characteristics of the new developed membranes are, when compared to previously reported values. Hydrophilic additives like poly(vinyl pyrrolidone) are frequently added to casting solutions to make membranes more hydrophilic. However, hydrophilic additives are frequently soluble and washed out during long time operation. Incorporation of hydrophilic groups by click chemistry is much better controlled and stable alternative.

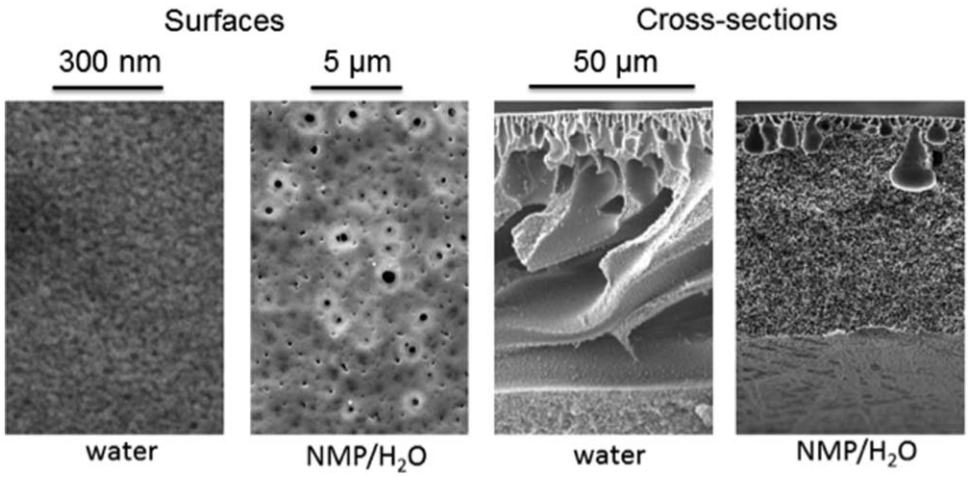

Figure 7. Morphology of surfaces and cross sections of membranes prepared from PSU-$TrN_{0.94}$ in water and NMP/H_2O (60/40).

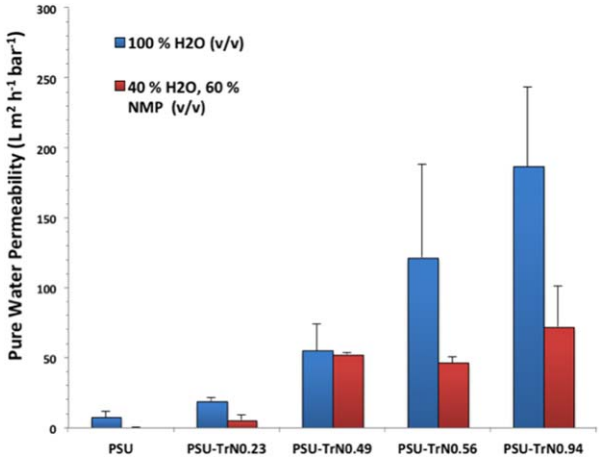

Figure 8. Pure water permeability of the fabricated membranes from different polymers and coagulation baths. [Color figure can be viewed in the online issue, which is available at wileyonlinelibrary.com.]

In long filtration experiments with albumin solutions, fouling becomes evident. This is a common effect in ultrafiltration membranes. Apart from numerous attempts and strategies to minimize fouling, it can hardly be completely avoided. Important is how much the water flux can be recovered after simple washing procedure or how reversible fouling is. To evaluate the antifouling properties of our developed membranes, a three-step filtration protocol adopted by many studies[15,40,41] was employed. It included pure water permeation of pristine membranes, BSA solution filtration, and pure water permeation of cleaned membranes. Resistance-in-series model[42] was used to describe the fouling mechanism and compare the membrane performance. According to this model, the fouling layer formed by protein adsorption during the filtration introduces additional hydraulic resistances on the feed side to the transport across the membrane, leading to flux decline. The hydraulic resistances caused by BSA fouling are determined by the following equations:

$$J_{w1} = \frac{\Delta P}{\eta_w R_m} \tag{3}$$

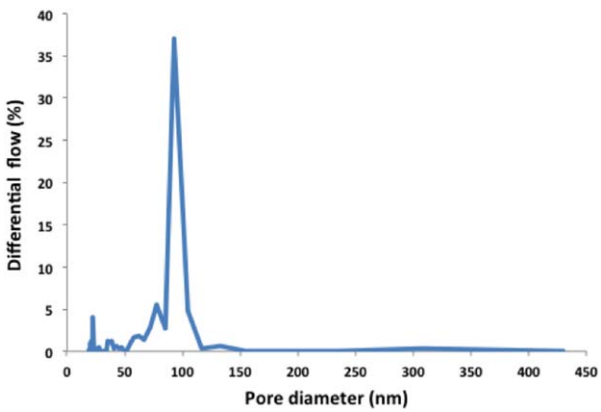

Figure 9. Pore size distribution of membrane prepared from PSU-TrN$_{0.94}$ in NMP/H_2O. [Color figure can be viewed in the online issue, which is available at wileyonlinelibrary.com.]

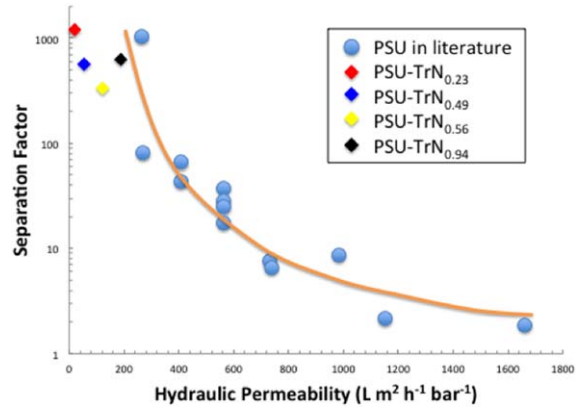

Figure 10. Separation factor-permeability trade-off curve for ultrafiltration polysulfone membranes using BSA. Light blue points reproduced from Mehta and Zydney.[39] [Color figure can be viewed in the online issue, which is available at wileyonlinelibrary.com.]

$$J_p = \frac{\Delta P}{\eta_w (R_m + R_r + R_{ir})} \tag{4}$$

$$J_{w2} = \frac{\Delta P}{\eta_w (R_m + R_{ir})} \tag{5}$$

where η_w is the viscosity of the permeate, which is 1.002×10^{-3} Pa S for water at 20°C; R_m, R_r, and R_{ir} denote the clean membrane hydraulic resistance, reversible fouling layer resistance, and irreversible fouling layer resistance, respectively. R_r and R_{ir} contribute to the total fouling resistance during the protein filtration. The value of R_r reflects the fouling caused by protein deposit on the membrane surface with a weak interaction, while R_{ir} shows the degree of fouling from permanent attachment of protein to the membrane, which cannot be removed by hydraulic cleaning process.

Figure 11 shows that the total fouling and especially irreversible fouling of membranes were clearly reduced with increased DF. It means membranes with higher DF are less prone to fouling and the fouling is more reversible, which enables higher extent of flux recovery. Furthermore if we take the amount of separated albumin protein into account, the normalized irreversible

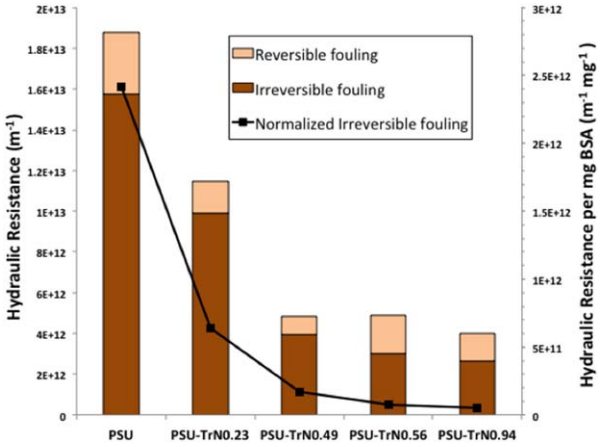

Figure 11. Reversible and irreversible fouling of the fabricated membranes from BSA filtration. [Color figure can be viewed in the online issue, which is available at wileyonlinelibrary.com.]

fouling resistance of unit BSA exhibits a stronger descending trend since the filtrate flux is increased with DF. The improved antifouling property of PSU membranes is attributed to the grafting of hydrophilic side-group to the polymer backbone, which forms a hydration layer to minimize the affinity of protein molecules to the surface.

CONCLUSIONS

We demonstrate how click chemistry can be used to address one of the most critical issues in membranes for water filtration: the flux reduction by fouling under operation. Well-controlled functionalization of PSU, by anchoring 1,2,3-triazole ring substituents containing OH groups to the backbone, successfully increased the hydrophilicity. Different DFs (23, 49, 56, and 94%) were achieved. The modified ultrafiltration membranes exhibited water permeability up to 187 L m^{-2} h^{-1} bar^{-1}. The modification reduced the extent of irreversible fouling during filtration of bovine serum albumin proteins while keeping high protein rejection ratio (>99%). This is one of many approaches, which can be followed by applying click chemistry to membrane developments. The membranes described in this work are now being further functionalized by promoting grafting reaction starting from the functionalized group, further tailoring the fouling resistance by growing hydrophilic brush segments or adding specific functionalities.

ACKNOWLEDGMENTS

The work was partially funded by the KAUST Competitive Research Grant program (CRG2).

REFERENCES

1. Hancock, L. F.; Kishbaugh, A. J.; Parham, M. E. US Pat., US5700902, **1997**.
2. Dizman, C.; Tasdelen, M. A.; Yagci, Y. *Polym. Int.* **2013**, *62*, 991.
3. Rose, J. B. *Polymer* **1974**, *15*, 456.
4. Susanto, H.; Stahra, N.; Ulbricht, M. *J. Membr. Sci.* **2009**, *342*, 153.
5. Tang, Z.; Qiu, C.; McCutcheon, J. R.; Yoon, K.; Ma, H.; Fang, D.; Lee, E.; Kopp, C.; Hsiao, B. S.; Chu, B. *J. Polym. Sci. B Polym. Phys.* **2009**, *47*, 2288.
6. Zornoza, B.; Irusta, S.; Tellez, C.; Coronas, J. *Langmuir* **2009**, *25*, 5903.
7. Yang, Y.; Shi, Z.; Holdcroft, S. *Macromolecules* **2004**, *37*, 1678.
8. Rahimy, M. H.; Peyman, G. A.; Chin, S. Y.; Golshani, R.; Aras, C.; Borhani, H.; Thompson, H. *J. Drug Targeting* **1994**, *2*, 289.
9. Johnson, B. C.; Yilgor, I.; Tran, C.; Iqbal, M.; Wightman, J. P.; Lloyd, D. R.; McGrath, J. E. *J. Polym. Sci. Polym. Chem. Ed.* **1984**, *22*, 721.
10. Rana, D.; Matsuura, T. *Chem. Rev.* **2010**, *110*, 2448.
11. Yilmaz, G.; Toiserkani, H.; Demirkol, D. O.; Sakarya, S.; Timur, S.; Torun, L.; Yagci, Y. *Mater. Sci. Eng. C* **2011**, *31*, 1091.
12. Cho, Y. H.; Kim, H. W.; Nam, S. Y.; Park, H. B. *J. Membr. Sci.* **2011**, *379*, 296.
13. Zhao, C.; Xue, J.; Ran, F.; Sun, S. *Prog. Mater. Sci.* **2013**, *58*, 76.
14. Ulbricht, M.; Belfort, G. *J. Membr. Sci.* **1996**, *111*, 193.
15. Zhao, Y.-F.; Zhu, L.-P.; Yi, Z.; Zhu, B.-K.; Xu, Y.-Y. *J. Membr. Sci.* **2013**, *440*, 40.
16. Cho, Y. H.; Kim, H. W.; Nam, S. Y.; Park, H. B. *J. Membr. Sci.* **2011**, *379*, 296.
17. Yue, W.-W.; Li, H.-J.; Xiang, T.; Qin, H.; Sun, S.-D.; Zhao, C.-S. *J. Membr. Sci.* **2013**, *446*, 79.
18. Park, J. Y.; Acar, M. H.; Akthakul, A.; Kuhlman, W.; Mayes, A. M. *Biomaterials* **2006**, *27*, 856.
19. Yi, Z.; Zhu, L.-P.; Zhao, Y.-F.; Zhu, B.-K.; Xu, Y.-Y. *J. Membr. Sci.* **2012**, *390-391*, 48.
20. Kolb, H. C.; Finn, M. G.; Sharpless, K. B. *Angew. Chem. Int. Ed.* **2001**, *40*, 2004.
21. Fournier, D.; Hoogenboom, R.; Schubert, U. S. *Chem. Soc. Rev.* **2007**, *36*, 1369.
22. Mansfeld, U.; Pietsch, C.; Hoogenboom, R.; Becer, C. R.; Schubert, U. S. *Polym. Chem.* **2010**, *1*, 1560.
23. Binder, W. H.; Sachsenhofer, R. *Macromol. Rapid Commun.* **2007**, *28*, 15.
24. Liu, F.; Hu, J.; Liu, G.; Hou, C.; Lin, S.; Zou, H.; Zhang, G.; Sun, J.; Luo, H.; Tu, Y. *Macromolecules* **2013**, *46*, 2646.
25. Hou, C.; Hu, J.; Liu, G.; Wang, J.; Liu, F.; Hu, H.; Zhang, G.; Zou, H.; Tu, Y.; Liao, B. *Macromolecules* **2013**, *46*, 4053.
26. Dimitrov, I.; Takamuku, S.; Jankova, K.; Jannasch, P.; Hvilsted, S. *Macromol. Rapid Commun.* **2012**, *33*, 1368.
27. Dimitrov, I.; Takamuku, S.; Jankova, K.; Jannasch, P.; Hvilsted, S. *J. Membr. Sci.* **2014**, *450*, 362.
28. Davis, K. A.; Charleux, B.; Matyjaszewski, K. *J. Polym. Sci. Part A Polym. Chem.* **2000**, *38*, 2274.
29. Avram, E.; Butuc, E.; Luca, C.; Druta, I. *J. Macromol. Sci. Part A* **1997**, *34*, 1701.
30. Gaina, C.; Gaina, V.; Ionita, D. *Polym. Int.* **2011**, *60*, 296.
31. Toiserkani, H.; Yilmaz, G.; Yagci, Y.; Torun, L. *Macromol. Chem. Phys.* **2010**, *211*, 2389.
32. Peinemann, K.-V.; Abetz, V.; Simon, P. F. W. *Nat. Mater.* **2007**, *6*, 992.
33. Hancock, L. F. *J. Appl. Polym. Sci.* **1997**, *66*, 1353.
34. Socrates, G. Infrared Characteristic Group Frequencies: Tables and Charts, 2nd ed.; Wiley: Chichester, **1994**.
35. Camacho-Zuniga, C.; Ruiz-Trevino, F. A.; Hernandez-Lopez, S.; Zolotukhin, M. G.; Maurer, F. H. J.; Gonzalez-Montiel, A. *J. Membr. Sci.* **2009**, *340*, 221.
36. Avram, E.; Brebu, M. A.; Warshawsky, A.; Vasile, C. *Polym. Degrad. Stab.* **2000**, *69*, 175.
37. McKelvey, S. A.; Koros, W. J. *J. Membr. Sci.* **1996**, *112*, 29.
38. Yang, Y.; Wang, P. *Polymer* **2006**, *47*, 2683.
39. Mehta, A.; Zydney, A. L. *J. Membr. Sci.* **2005**, *249*, 245.
40. Wang, Y.-q.; Wang, T.; Su, Y.-l.; Peng, F.-b.; Wu, H.; Jiang, Z.-y. *Langmuir* **2005**, *21*, 11856.
41. Zhu, L.-P.; Dong, H.-B.; Wei, X.-Z.; Yi, Z.; Zhu, B.-K.; Xu, Y.-Y. *J. Membr. Sci.* **2008**, *320*, 407.
42. Juang, R.-S.; Chen, H.-L.; Chen, Y.-S. *Sep. Purif. Technol.* **2008**, *63*, 531.